Title
AXIAL DISPERSION IN LIQUID FLOW THROUGH PACKED BEDS

Authors
Miller, Steven Frank
King, C.Judson.

Publication Date
1965-05-24

UCRL-11951

University of California

Ernest O. Lawrence Radiation Laboratory

AXIAL DISPERSION IN LIQUID FLOW THROUGH PACKED BEDS

Berkeley, California

DISCLAIMER

Research and Development

UCRL-11951

UNIVERSITY OF CALIFORNIA

Lawrence Radiation Laboratory
Berkeley, California

AEC Contract No. W-7405-eng-48

AXIAL DISPERSION IN LIQUID FLOW THROUGH PACKED BEDS

Steven Frank Miller and C. Judson King

May 24, 1965

AXIAL DISPERSION IN LIQUID FLOW THROUGH PACKED BEDS

Contents

AXIAL DISPERSION IN LIQUID FLOW THROUGH PACKED BEDS

Steven Frank Miller and C. Judson King

Department of Chemical Engineering
Lawrence Radiation Laboratory
University of California
Berkeley, California

May 24, 1965

ABSTRACT

Step-function injection and purging of a dilute salt tracer in water was used to measure axial dispersion for low Reynolds number liquid flow through beds of uniform sized, random packed glass spheres. The resultant data and those of several previous studies are coordinated and interpreted in terms of Reynolds number, Schmidt number, and Peclet number.

I. INTRODUCTION

Axial dispersion in laminar liquid flow through beds of solids is important for several engineering applications, including ion exchange and miscible displacement in petroleum reservoirs. The present work concerns experimental measurements of axial dispersion during liquid flow in the range of Reynolds numbers between 0.003 and 40 and interpretation of the results in the light of past studies. The work was undertaken because of the importance of this flow range, because of wide discrepancies in the available data and because of the lack of an accepted theoretical explanation of dispersion behavior under these conditions. A particular effort was made to discern any independent effect of particle size.

Many previous studies have been made of axial dispersion during fluid flow through beds of particulate silids. The recent review of Perkins and Johnston[18] is particularly comprehensive in reporting and analyzing past work. The results of these various investigations have commonly been interpreted in terms of an axial Peclet number, $d_p U/E'$, containing a linear interstitial dispersion coefficient, E', and the mean linear interstitial velocity, U. The Peclet number may also be defined as $d_p U_o/E$ with no resulting change in magnitude if U_o is the superficial fluid velocity (ϵU) and E is the axial dispersion coefficient based on the open bed ($\epsilon E'$). E and E' are equivalent to effective axial diffusivities if a diffusion model is obeyed. Furthermore, Peclet number can be conceived as the ratio of material transport by axial convection to the net material transport by axial dispersion (i.e., the greater the importance of axial dispersion relative to convection, the smaller the Peclet number).

In the case of liquid flow there is considerable disagreement between the avialable sets of data relating the axial Peclet number to the Reynolds number of flow. Jacques, Hennico, Moon and Vermeulen[13] have pointed out that a general feature is an increase in Peclet number as the flow undergoes a transition from laminar to turbulent flow. In the region of laminar flow ($Re < 10$) the available data indicate that the Peclet number for liquids becomes relatively insensitive to changes

in Reynolds number.[1,3,6-9,13,15,19,21,24,26] There is, however, no consensus concerning the absolute magnitude of the Peclet number in this region, a fact which is confirmed by recent reviews.[4,13,18,23] Some of the discrepancies may come from the use of irregular particles which are difficult to characterize and from marked changes in fluid physical properties across a displacement front. It has also been suggested that there is an effect of particle size beyond that represented by the Peclet and Reynolds groups.[5,6,18] This point is considered further in the present work

A. Effect of Schmidt Number

A comparison of past measurements indicates substantial difference in behavior between gas and liquid systems. Jacques, et al.[13] show that the product of Peclet number and voidage (ϵP) in liquid systems has a relatively constant value of 0.8-0.9 at values of N_{Re}' ($= N_{Re}/(1 - \epsilon)$) above 1000. At lower values of N_{Re}' there is a gradual decrease in ϵP until a nearly constant value of 0.2 is found for $N_{Re}' < 20$. McHenry and Wilhelm[16] in a study of gas systems also found ϵP to be about 0.8 at $N_{Re}' > 500$. On the other hand as N_{Re}' decreases their results indicate a slight reduction in ϵP around $N_{Re}' = 250$ followed by a return to the original high level of $\epsilon P = 0.8$ at still lower N_{Re}'.

McHenry and Wilheml noted that a relatively constant Peclet number near 2 was in accord with the hypothesis that complete mixing of the fluid occurred once every particle diameter. There is general agreement that turbulent eddies serve to keep the individual void spaces almost entirely mixed in the range of very high Reynolds number. Jacques, et al.[13] have extended this explanation by postulating a unique transition of ϵP downward for high Schmidt numbers toward another limiting value characteristic of segregation due to the laminar velocity distribution. Jacques, et al., and Perkins and Johnston[18] suggest that the transition occurs over a broad range as the turbulence within the various cells ceases to be strong enough to cause complete mixing and as cells of different sizes change from turbulent to laminar flow. Jacques,

et al., and Perkins and Johnston also suggest that the gas phase Peclet numbers rise again to the upper limiting value of ϵP after following the high Schmidt number curve for a short way because lateral molecular diffusion in the void spaces compensates for segregation due to laminar flow. Thus below $N_{Re}' = 100$ molecular diffusion is able to keep individual void spaces well mixed in gaseous systems. ϵP should then be constant at 0.8-0.9 for gases down to N_{Re}' on the order of 1 (for $N_{Sc} \simeq 1$), where axial molecular diffusion should cause a decrease in ϵP. A decrease in gas phase Peclet number at very low Reynolds numbers is convirmed by the results of Carberry and Bretton,[8] Sinclair and Potter[22] and Blackwell, et al.[4]

The only obvious basic difference between gas and liquid systems lies in the Schmidt number. The high Schmidt number of liquids should delay the effect of molecular diffusion in causing the mixing of individual void spaces until lower values of N_{Re}' and should cause the effect of axial molecular diffusion to be unimportant until N_{Re}' is on the order of $1/N_{Sc}$. A seeming paradox arises in that Jacques, et al., found ϵP essentially constant at the lower limiting value of 0.2 for $0.07 < N_{Re} < 0.8$, where one would expect the effect of molecular diffusion on void space mixing to have become important.

B. Effect of Particle Size

Another factor should be considered. High Reynolds number data have invariably been obtained for beds of larger particle sizes, while smaller particle sizes have been employed for low Reynolds number data. Klinkenberg and Sjenitzer[14] suggested the use of a packing or inhomogeneity factor, λ, which reflects differences in the geometric configuration of a bed. Complete mixing of individual void cells would then produce an axial Peclet number of $2/\lambda$. The concept has been adopted by several subsequent authors.[4,6,18,19] Klinkenberg and Sjenitzer report values of λ ranging from 1 to 4 for various conditions, while Perkins and Johnston[18] suggest that λ is a function of particle diameter,

ranging from 1 for regular packing and large particle size up to 10 for random packing of spheres and a particle diameter of 100 μ. Presumably the high value of λ for smaller particles represents more bridgings between particles and greater variations in local voidages which promote a channeling phenomenon.

It is also possible that a pertinent variable is the ratio of column diameter to particle diameter (d_t/d_p), even for values of this ratio above 20 where one normally expects significant column wall effects to be absent. Tompkins, et al.[25] report elution band widths for ion exchange at $N_{Re} = 0.06$ with a fixed particle size (40-60 mesh) and different column diameters. The results suggest that E varies as the 1/3 power of column diameter, which again could be the result of a channeling effect. It is interesting to note that the high Reynolds number of data of Jacques, et al.[13] were taken with (d_t/d_p) equal to 9 and 18, while the ratio was 1030 for the low Reynolds number data. Correction of the Peclet number by $(d_t/d_p)^{-1/3}$ would return the low Reynolds number data of Jacques, et al., to the higher ϵP limit.

Past data are inconclusive concerning an independent effect of d_p of d_t/d_p within a given study. Ebach and White[9] and Raimondi, et al.[19] found no discernable effect of particle diameter over a range of 0.1-7 mm. On the other hand, the data of Carberry and Bretton,[8] Liles and Geankoplis,[15] Stahel and Geankoplis,[23] Brigham, et al.[6] and Ampilogov, et al.[1] indicate that ϵP is altered by changes in d_p at fixed N_{Re}, but there is no consensus regarding the magnitude of the effect, nor does the effect appear to be well ordered.

The present study was made with spheres of four different uniform sizes, ranging from 0.05 to 1.4 mm.

II. APPARATUS

The experimental apparatus was built to conform with several general specifications:

a. The apparatus had to permit utilization of experimental techniques and column diameter to bead diameter ratios similar to those employed by Jacques, et al., in order to afford a comparison.

b. The apparatus had to be convenient for operation over a wide range of flow rates.

c. Some means was required for distinguishing between end effects and the axial mixing effects characteristic of a region in a relatively long bed.

A schematic of the apparatus is given in Fig. 1. Two constant head tanks were mounted 30 feet above the top of the column. One was filled with tap water and the other with a solution of 0.01 N $NaNO_3$ in tap water. The two tanks were connected to the injection system by 1/4-in. tygon lines.

The injection system consisted of two single pole, double throw, microvalves which were operated together. These connected one stream to the column while the other stream travelled through a variable resistance (in the form of a valve) to a drain. The flip of a single switch caused instant transposition of the streams. Runs were attempted with the variable resistance valve wide open and fully closed. Since the steps recorded inside the column were identical for these two cases, it was concluded that transients in flow between the head tank and the injection manifold could be neglected.

Glass columns, 1/2 in. I.D. and packed randomly with spheres, were employed for the dispersion studies. Downward flow was employed in the column because earlier experiments indicated a tendency of the bed to fluidize partially even at low N_{Re}'. Alternating runs were carried out with injection (addition of $NaNO_3$ solution) followed by purging (switching to flow from the tap water tank). Thus the denser fluid was alternately above and then below the less dense solution. In this way it was possible to observe any density or viscosity gradient effect which might influence axial mixing at very low N_{Re}'.

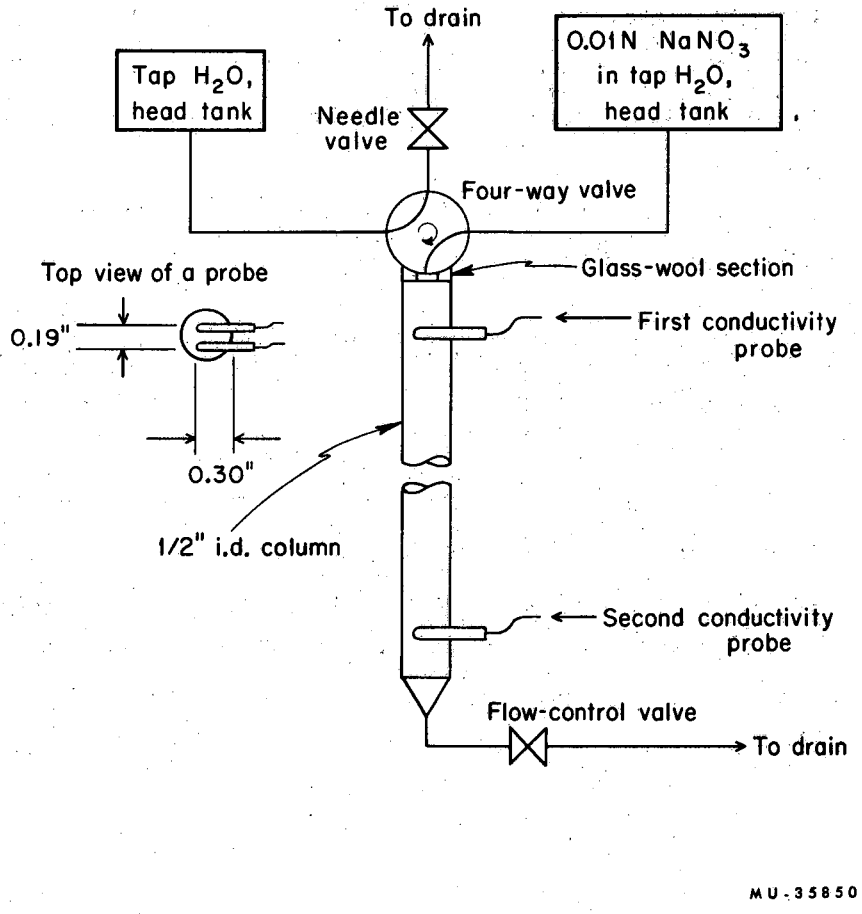

Fig. 1. Schematic of apparatus.

Below the microswitch injection point was a small slug of glass wool followed directly by the first two inches of column packing. At this point was located the first set of electrical conductivity probes.

The conductivity probes consisted of two parallel rhodium coated nickel pins lying in a plane perpendicular to the direction of flow. The probes were intended to be as similar in material and geometry to those used by Jacques, et al., as practically possible in the confined flow space of a 1/2-in. column. The cell arrangement here differs from that of Jacques, et al., in that the 1/16-in. rods entered the column through a Teflon plug mounted in the wall and were uncapped (but rounded) at their far end. The pins utilized by Jacques, et al., were also 0.30 in. long and about 0.188 in. apart, center to center, but were insulated at both ends.

Three columns were constructed, differing only in the distance between the two conductivity cells. The lengths of packed bed between cells were 22 inches, 11 inches, and 5-1/2 inches. Measurements made with two or more columns gave the ability to check for an effect of column length. The shorter columns gave higher flow rates and quicker breakthrough with a little less precision than the long column.

Below the second set of probes was another inch of packing, a screen, and finally a valve which was used to control the flow rate in the column.

The circuitry associated with the conductivity cells was basically the same as that employed by Jacques, et al. It had the additional features of a standard decade resistance box which could replace the conductivity cells in the circuit for rapid consistency checks, and also separate gain controls for each conductivity cell.

Four sizes of spheres were employed for the measurements. These included 50.8, 99, and 470 micron Scotchlite microspheres made by Minnesota Mining and Manufacturing Company. The fourth size was 1.4 mm glass spheres obtained from Jaymar Scientific, Inc., and donated by Bio-Rad Laboratories of Richmond, California.

III. EXPERIMENTAL PROCEDURE

The gains for each set of probes were adjusted so that they both yielded readings having the same upper and lower bounds. The recorder chart speed was then set so that the breakthrough curves had close to 45° midpoint slopes to minimize errors in analysis.

The microvalve arrangement was then used to cause a step change in the concentration of the flowing stream without permitting any variation of flow rate. The breakthrough at the upper cell was recorded and then the channels were switched to monitor the breakthrough at the lower cell. The degeneration of the step which had taken place between these two cells was assumed to be free of end effects. This procedure was repeated three more times so that two injections and two purges were recorded. Then Peclet numbers were calculated for each of the four runs and were later averaged to give a single datum point. Any realistic nonlinearity would have affected Peclet numbers for injection and purge in opposite ways. A careful comparison was made of the four runs which made up each datum point to detect any significant differences between injection and purge. This gave a built-in safegaurd against a variety of experimental errors.

IV. CALCULATION OF DATA

Peclet numbers were computed using the random walk model, following the procedure adopted by Jacques, et al. For large column Peclet numbers it becomes impossible to distinguish experimentally between the predictions of most of the models which have been suggested. The random walk model predicts that

$$N = 4\pi S^2 - 0.80 \tag{1}$$

where S is the dimensionless midpoint slope of the breakthrough curve and N is the resulting column Peclet number.[12] Then simple division of N by the ratio of column height to particle diameter yields the "Packing Peclet number", P, which is the quantity of interest. Since the smallest N ever considered is about 400 it is apparent that no noticeable error results from disregarding the 0.80 constant.

Since the computations involved the difference in degree of degeneration of a step at two different points in the appraturs precise measurements were required. The final forms of the equations used to evaluate the experimental data were

$$P = \frac{4\pi \epsilon d_p}{L} \frac{(\Delta h)^2}{\left(\frac{a_2}{\tan \theta_2}\right)^2 - \left(\frac{a_1}{\tan \theta_1}\right)^2} \tag{2}$$

and

$$N_{Re}' = \frac{\epsilon}{1 - \epsilon} L \frac{d_p X}{\nu \cdot \Delta h} \tag{3}$$

where ϵ is void fraction, L is the distance between conductivity cells, d_p is the particle diameter, ν is the kinematic viscosity of tap water, and X the recorder chart speed. Δh, a_1, $\tan \theta_1$, a_2 and $\tan \theta_2$ must all be measured graphically from the breakthrough recordings. a_1 and a_2 are the amplitude of the step recorded at the upper and lower cells respectively; $\tan \theta_1$ and $\tan \theta_2$ are the respective midpoint slopes; and Δh is the chart distance between breakthrough

curve midpoints. Void fractions were measured in a 1/2-in. I.D. by 2 ft tubular glass container constructed specifically for that purpose. ϵ was always close to 0.39.

Equation (2) was arrived at in the following manner. For any uniform packing medium Eq. (1), neglecting the constant, indicates that

$$N = 4\pi \left\{ \frac{h}{a} \cdot \tan \theta \right\}^2 \tag{4}$$

where h is the elapsed recorder chart distance between an initial perfect inlet step and the midpoint of the response measured at some point in the bed. a is the chart height of the response and $\tan \theta$ is the midpoint slope of the response in chart units. Since

$$L = \frac{hU}{X} \quad , \tag{5}$$

a combination of Eqs. (4) and (5) with the definition N yields

$$\left(\frac{a}{\tan \theta} \right)^2 = 4\pi X \cdot \left(\frac{d_p}{UP} \right) \cdot h \tag{6}$$

Since the left hand side of Eq. (6) is linear in h, it is apparent that for the region between any two monitored points in the bed

$$\Delta \left(\frac{a}{\tan \theta} \right)^2 = 4\pi X \cdot \left(\frac{d_p}{UP} \right) \cdot \Delta h \tag{7}$$

Furthermore, as long as the response at the two locations is a true degenerate step in shape and the bed is uniform between the two locations, Eq. (7) will apply no matter what sort of packing caused the degeneration of the step before the first probe. Equation (7) leads directly to Eq. (2).

Initially rotameter and drop collection techniques were employed to determine flow rates, but calculation of the time between midpoints of the breakthrough curves on the recorder chart turned out to be the most efficient method of all. Material balance checks for injection

and purging confirmed that the time interval between midpoints agreed within 2% with flow rates measured by the other means.

Further details concerning the experimental conditions are available in Appendix II.

V. RESULTS

The response curves did not show a marked amount of asymmetry; the shapes were similar to the predictions of the random walk model and the segmented laminar flow model at high column Peclet numbers.[12] There was a small amount of tailing, but not in sufficient amount to have any apparent effect on the midpoint slope. On this basis any policy of allowing for the presence of dead spaces in the bed should have no influence on the analysis of the data.

The experimental results obtained for different bead sizes and bed lengths are shown in Fig. 2. As indicated earlier, each datum point is the result of averaging two injection and two purge Peclet numbers, taken at the same N_{Re}'. The brackets associated with each point denote the range of the individual Peclet numbers composing that point. In the cases of the 1.4 mm and 470 μ glass beads the individual Peclet numbers examined before the averaging process was performed showed very little spread. As bead diameter decreased the precision also seemed to decrease, especially at very low Reynolds numbers. The entrance section before the beads themselves was arranged and packed in a similar fashion for all bead sizes and thus resulted in a fairly constant amount of degeneration in the step function. However, the packed length between cells caused less and less step degeneration as d_p decreased. As a result, the fraction of the total degeneration taking place between probes decreased significantly with d_p so as to affect the precision, but not necessarily the accuracy, of the results.

From the data the following trends were uncovered:

a. The end of the fall in Peclet number due to the transition from turbulent to laminar flow was observed. Figure 3 demonstrates

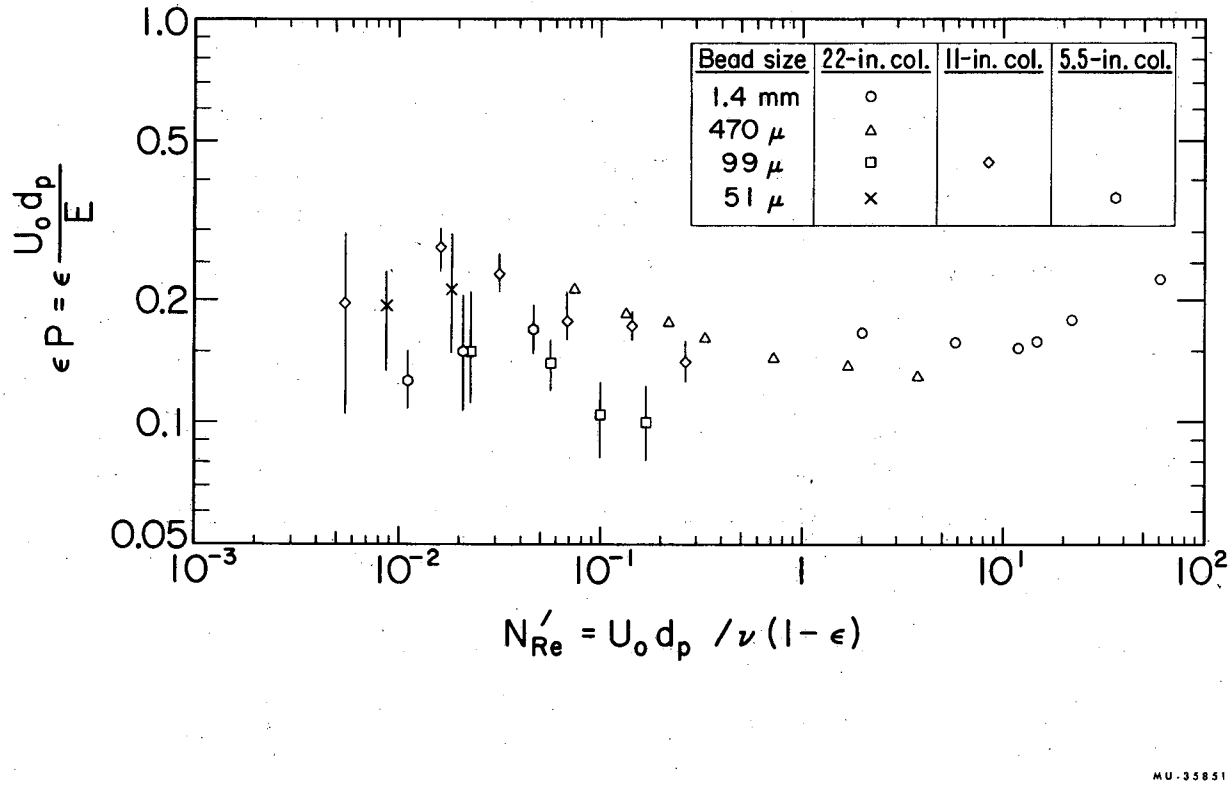

Fig. 2. Experimental results.

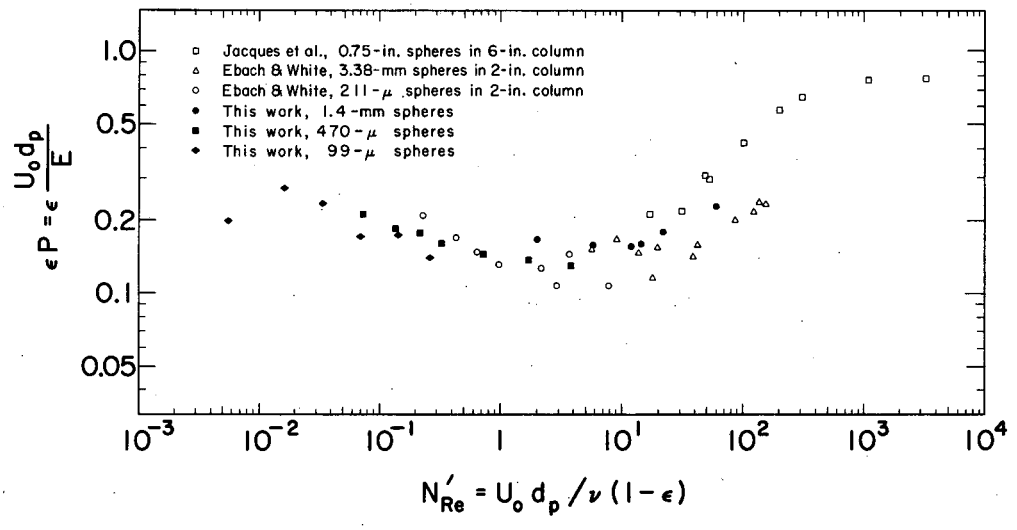

Fig. 3. Comparison with data of Jacques, et al. and Ebach and White.

that the effect observed lies between the data of Jacques et al.[13] and the data of Ebach and White,[9] and that all three sets are in acceptable agreement. Frequency response data of Ebach and White for two sphere sizes are included in Fig. 3. These are representative of the remainder of their data.

b. As Reynolds number decreases the Peclet number passes through a minimum near $N_{Re}' = 10$ and then rises with a slope of about -1/6. The data of Ebach and White also experience a minimum Peclet number in this region and then rise with a similar slope.

c. At still lower Reynolds numbers, below $N_{Re}' = 0.02$, the Peclet number exhibits a maximum and begins to fall. This fall was echoed in the 50.8 μ data taken in the 22" and 5-1/2" columns.

d. Data for 99 μ beads with a 22-in. bed length fall below those for 99 μ beads with an 11-in. bed length. However, data for 50.8 μ beads and a 22-in. bed length fall above those for 50.8 μ beads and a 5-1/2-in. bed length. It was concluded that no major length effect existed.

e. Examination of data for 99 μ, 470 μ, and 1.4 mm glass beads reveals no strong trend of Peclet number with either particle diameter or with the ratio of bed diameter to particle diameter. The very small decrease of Peclet number with particle diameter is within the calculational error due to assigning a nominal uniform particle diameter. Microscopic examination revealed that there was a range of bead sizes composing each set of Microspheres as supplied by the manufacturer.

VI. DISCUSSION OF RESULTS

A packed bed may be thought of as a series of main voids interconnected by smaller voids or channels so as to form a three dimensional network. In a randomly packed bed these main voids are irregular in shape and are distributed about a certain effective size. When the main voids are well mixed (of uniform concentration) and are interconnected by convection only, a mixing cell type of model may be applied to the system with the size and spacing of cells on the order of d_p. Although the main voids are larger than the interconnecting channels they have a lower average velocity. As a result eddy or molecular diffusion can cause appreciable mixing in the main voids without producing an amount of diffusion between cells which is significant in comparison to the convective transport in channels. However, when diffusion in the interconnecting channels is significant in relation to convection the picture of isolated, well mixed void cells must break down. The effect of diffusional mixing will be to bring about a larger effective mixing cell size. Whenever the effective size of a mixing cell increases, Peclet number decreases.

In the case of laminar flow and infinite Schmidt number, in the absence of both eddy and molecular diffusion, fluid mixing is still achieved when fluid filaments are forced together and are then split by geometry in such a way as to transfer some fluid from one filament to the other and thereby cause a velocity change. This mixing mechanism should give an effective mixing cell size and spacing substantially larger than d_p, but should produce a Peclet number independent of Reynolds number.[12]

At high Reynolds numbers ($N_{Re}' > 1000$) flow is turbulent with the main voids well mixed by the eddies which are generated. Therefore, a mixing cell model applies closely and ϵP is constant with respect to Reynolds number. If a single sequence of cells is postulated, the fact that ϵP is equal to 0.8-0.9 implies that the cell spacing in the axial direction is 2.5 ϵd_p. The transition to laminar flow takes place over at least two decades of N_{Re}'. In this region behavior is dictated by

the Schmidt number of the system. If N_{Sc} were infinite the only mixing mechanism after eddy diffusion damped out would be the filament mixing mentioned previously. The Peclet number would drop to a plateau characteristic of that mechanism and remain there for all smaller N_{Re}' greater than zero.

A. Dispersion in Gases

For low N_{Sc} (on the order of 1), as the transition from fully turbulent to laminar flow begins, molecular diffusion soon becomes strong enough in relation to throughput to aid the remaining eddies in keeping the main voids mixed. Such an interaction of eddy and molecular diffusion mechanisms can explain the small dip and rapid return of the data of McHenry and Wilhelm[16] to $\epsilon P = 0.8\text{-}0.9$, as shown in Fig. 4. At still lower Reynolds numbers axial diffusion between voids must break down the isolated mixing cells and eventually yield the behavior expected from dispersion governed solely by axial molecular diffusion. The gas phase data of Carberry and Bretton[8] were obtained for the dispersion of an air tracer in helium, for which $N_{Sc} = 1.7$. Their data are presented in Fig. 4, with the Reynolds numbers recomputed on the basis of the viscosity of helium rather than air. It may be seen that the data agree well with an asymptotic line for $N_{Sc} = 1.7$, based on dispersion due to axial molecular diffusion alone with a tortuosity factor of $\sqrt{2}$ and a void fraction if 0.40[13]

$$\epsilon P = 0.85\, N_{Sc}\, N_{Re}' \qquad (8)$$

Blackwell, et al.[4] also found close agreement with Eq. (8) for the dispersion of a helium tracer in argon.

The region of transition between the extremes of axial molecular diffusion control on the one hand and the isolated mixed cell model giving $\epsilon P = 0.8\text{-}0.9$ on the other hand is covered by the data of Sinclair and Potter,[21] who studied the dispersion of a mercury tracer in air.

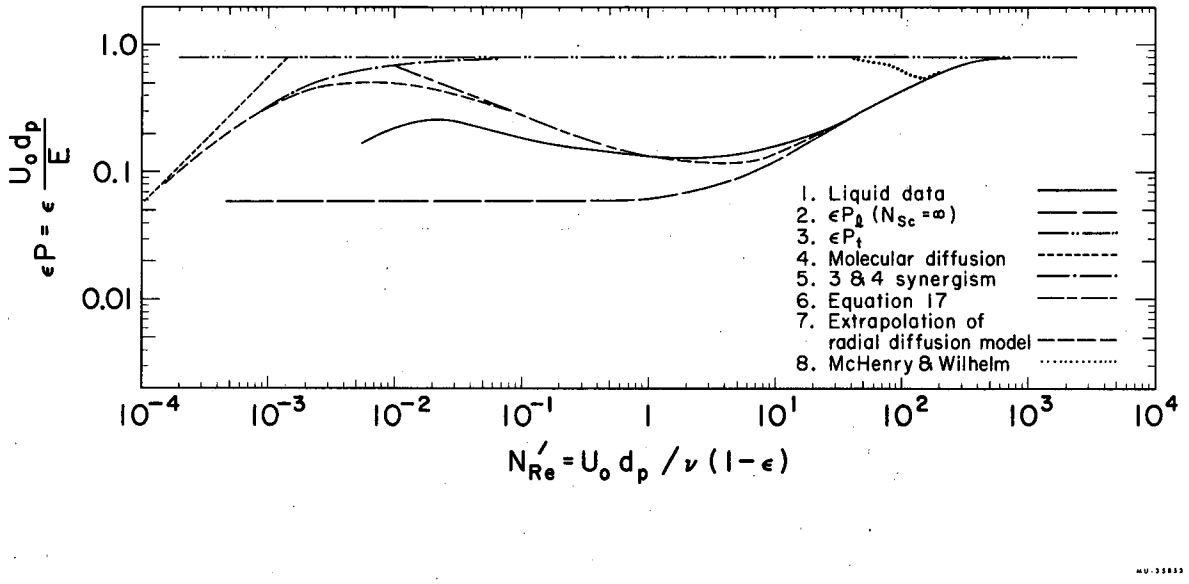

Fig. 4. Predicted effect of Schmidt or Prandtl number.

For their system N_{Sc} should be about 1.2, as reported by them and as computed from Lennard-Jones force constant data.[20] At high Reynolds numbers their results give ϵP constant at about 0.95, in agreement with the results of McHenry and Wilhelm. At lower Reynolds numbers the Peclet number falls off and seems to approach the axial diffusion asymptote slowly. The beginning of the drop in Peclet number does not appear to be more than one decade in Reynolds number above the intersection of the asymptotes.

B. Mass Dispersion in Liquids

The data for the present experiment were obtained for a system where $N_{Sc} = 730$. This value is calculated for 20°C from the ionic mobilities of Harned and Owen.[11] Because of the high Schmidt number, as N_{Re}' decreases, ϵP follows the infinite Schmidt number curve for a greater distance than do the data for N_{Sc} near 1. At sufficiently low N_{Re}' radial mixing by diffusion within the main void cells becomes important and causes an increase in ϵP as N_{Re}' is further reduced. However, for $N_{Sc} = 730$ the Reynolds number at which molecular diffusion becomes important is so low that there are few turbulent eddies, if any, remaining to interact with molecular diffusion and speed complete mixing in the main voids. As a result the return toward the extreme of well mixed cells is more gentle and further delayed with respect to the data for gas phase dispersion.

The nature and location of the rise in ϵP due to increasing mixing of the main voids by molecular diffusion can be interpreted in the following extremely oversimplified way:

In laminar flow a certain amount of mixing occurs from the geometric blending and splitting of fluid filaments which characterizes the lower limiting value of ϵP for $N_{Sc} \to \infty$. Any additional mixing within the main voids must occur through diffusional mass transfer between the various fluid streams entering a void cell. Figure 5(a) portrays two streams flowing into a common packing void and splitting

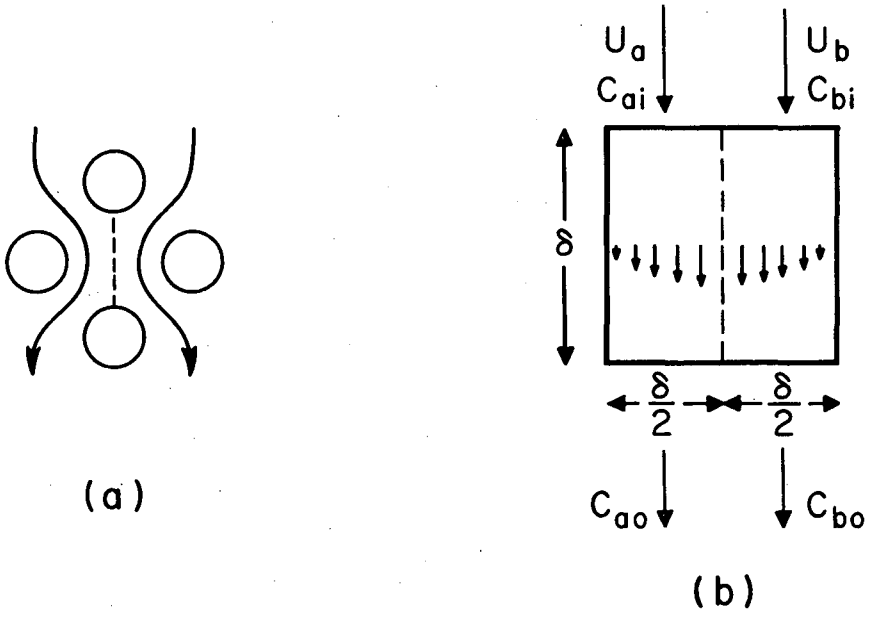

Fig. 5. Cell diffusion model.

apart again. Consider the effects on axial dispersion of radial mass transfer within a void space with short fluid contact times.

Let E_m be the efficiency of mixing in voids by diffusion over and above the geometrical stream blending and splitting of filaments in laminar flow. Then

$$\epsilon P = \epsilon P_\ell + E_m \left(\epsilon P_t - \epsilon P_\ell \right) \quad , \tag{9}$$

where ϵP_t is the Peclet number for total mixing in void cells and ϵP_ℓ is the Peclet number for infinite N_{Sc} in the laminar regime. The configuration shown in Fig. 5(a) will be reduced to a cube of side δ, pictured in Fig. 5(b), in order to derive the simplest possible model for a meaningful qualitative picture. The two entering streams are assumed to be of equal volume and velocity, and each enters the cell with a uniform concentration; however the two streams have different concentrations from one another. The efficiency of mixing can be equated to the approach to equilibrium in the cell, and can thus be defined as

$$E_m = 1 - \frac{C_{ao} - C_{bo}}{C_{ai} - C_{bi}}$$

$$= \frac{2(C_{ai} - C_{ao})}{C_{ai} - C_{bi}} \tag{10}$$

Furthermore,

$$C_{ai} - C_{ao} = \frac{K_L \, \delta (C_{ai} - C_{bi})}{u \, \delta / 2} \quad , \tag{11}$$

where u is the average velocity of either stream and K_L is the overall mass transfer coefficient based on the initial driving force. Therefore

$$E_m = \frac{4 K_L}{u} \tag{12}$$

Since the average individual mass transfer coefficient for either stream, k_{L_m}, will be twice K_L,

$$E_m = \frac{2k_{L_m}}{u} \tag{13}$$

The velocity of the imaginary interface between the two streams in the void cell is defined as $u_S = nu$. n will probably lie between 1 and 3, depending upon what velocity profile applies to the void cell and whether or not the interface falls at the point of maximum velocity. As long as $E_m < 0.5$, a penetration model should describe the mass transfer, yielding

$$k_{L_m} = 2\sqrt{\frac{Du_S}{\pi\delta}} \tag{14}$$

where D is molecular diffusivity. It follows directly that

$$E_m = 4\sqrt{\frac{n\,D}{\pi u\delta}}\ , \tag{15}$$

and assuming $u = u_o/\epsilon$ and defining $\delta = d_p/m$ results in

$$E_m = 4\sqrt{\frac{nm}{\pi}}\left(\frac{D\,\epsilon}{U_o\,d_p}\right)^{1/2}$$

$$= 4\sqrt{\frac{nm\epsilon}{\pi(1-\epsilon)}}\left(N_{Sc}\right)^{1/2}\left(N_{Re}'\right)^{-1/2} \tag{16}$$

If m is taken to be 1, n is taken to be 2, and $\epsilon = 0.4$, the multiplicative constant in Eq. (16) will become 2.6. Applying Eq. (16) to the system used in this experiment where $N_{Sc} = 730$ yields

$$E_m = 0.096\left(N_{Re}'\right)^{-1/2} \tag{17}$$

and

$$\epsilon P = \epsilon P_\ell + 0.096\left(N_{Re}'\right)^{-1/2}\left(\epsilon P_t - \epsilon P_\ell\right) \tag{18}$$

Figure 4 shows approximations for ϵP_t and ϵP_ℓ along with the consequent curve of ϵP vs N_{Re}' predicted by Eq. (18). ϵP_t is taken constant at 0.8 until N_{Re}' becomes low enough for axial molecular diffusion to become important. The transition of ϵP_t toward the asymptote of axial molecular diffusion control is obtained by taking the E involved in $\epsilon P = 0.8$ at any N_{Re}' to be additive with a superficial molecular diffusions contribution equal to $\epsilon D/\sqrt{2}$. ϵP_ℓ follows the infinite Schmidt number curve during the transition from turbulent to laminar flow, and is assumed to line out at $\epsilon P_\ell = 0.06$ in the fully laminar region. The rise in ϵP due to Eq. (18) is significant for $N_{Re}' > 10$. Above $\epsilon P = 0.4$ where $E_m > 0.5$ the penetration mass transfer model breaks down and E_m is lower than predicted by Eq. (18). The dashed curve represents a reasonable transition between Eq. (18) and the upper limit of ϵP_t.

Although the rise in ϵP due to Eq. (18) is somewhat sharper than the rise of the observed data it is apparent that Eq. (18) provides a better representation of the rise than does the model of Taylor dispersion in a long capillary of uniform diameter. The capillary model requires a variation ϵP with $(N_{Re}')^{-1}$,[2,13] which is much steeper than the observed data and the prediction of Eq. (18). For any reasonable values of n and m Eqs. (16) and (18) will succeed in locating the value of N_{Re}' at which the rise due to radial cell mixing begins, whereas a capillary model does not.

According to Eq. (16) the gas phase data of McHenry and Wilhelm should not show an appreciable upward rise away from the infinite Schmidt number curve above $N_{Re}' = 30$. As noted earlier, however, the return of ϵP to the upper limit for well mixed cells in the case of gases is attributable to both eddy and molecular diffusion. A given amount of molecular diffusion will cause more mixing of individual void cells at low Schmidt numbers because partial mixing by eddies reduces the distances over which molecular diffusion must act. This explanation also suggests that the ϵP curve for $N_{Sc} = 730$ should be raised somewhat above the prediction of Eq. (18) in the range $1 < N_{Re}' < 50$ as shown by the solid curve in Fig. 4. To the extent that turbulence remains

in the main void cells in this region it will provide a synergistic effect with molecular diffusion for cell mixing.

The present data show that ϵP ceases to rise with decreasing Reynolds number and probably begins to fall again below $N_{Re}' = 0.01$ The maximum value of ϵP attained is approximately 0.27. It is logical to presume that this leveling out and subsequent fall is the result of axial molecular diffusion in the connecting channels. The maximum in ϵP seems to occur about two decades in N_{Re}' above the intersection of the extrapolated data with the asymptote for axial molecular diffusion control. A transition beginning approximately one decade in N_{Re}' above the intersection of asymptotes is predicted by the assumption that E from a mixing cell model is directly additive with $\epsilon D/\sqrt{2}$ in causing dispersion in the transition region between the two extremes; however the assumption of direct additivity has no real physical justification.

Another factor should be considered. A certain amount of local fluid heating may have occurred in the present system in the vicinity of the two sets of electrodes. This heating could give rise to additional mixing by means of relatively large natural convection patterns. The effect would be to give a deceptively low value of ϵP, and the behavior would be most pronounced at the lower velocities. On the other hand, the results of Ebach and White[9] were obtained using a colorimetric technique and show the same leveling off and possible drop in ϵP at approximately the same N_{Re}' as in the present study. N_{Sc} for their system should have been still greater than in the present work.

One possibility, therefore, is that molecular diffusion in the connecting channels begins to become important before molecular diffusion in the main void cells has succeeded in achieving complete mixing of those cells. Since molecular diffusion is independent of local geometry and since the molecular diffusivity is a constant throughout the bed, it is reasonable to expect that when molecular diffusivity becomes strong enough to mix a void to a given degree, it has also become strong enough to mix the connecting channels axially to a corresponding degree

which is a function of packing geometry alone. The efficiency of mixing in the main voids at the point where axial molecular diffusion in the channels begins to become important is indicated by the ratio of the maximum value of ϵP in the laminar region to ϵP_t. Therefore, while N_{Re} for the maximum laminar flow ϵP should be a function of N_{Sc}, the laminar maximum ϵP itself should be a function of bed geometry only.

For gas phase dispersion one would expect the same maximum ϵP (approximately 0.27) to occur before the drop due to axial molecular diffusion if the diffusivity in the channels and voids is independent of position in the bed and if ϵP_t is the same as at lower Reynolds numbers. However, the turbulent "effective" diffusivity may be greater in the larger voids than in the channels (greater maximum scale of turbulence) and, therefore, it is possible that the main voids could become well mixed while eddy diffusion in the channels is still unable to compete with convection. Since the values of ϵP found by Sinclair and Potter remain high nearly to the point of intersection of asymptotes at $N_{Re}' = 1$ this argument requires that some turbulence be present in the void spaces down to $N_{Re}' = 1$.

The differences between the maximum values of ϵP for gas and liquid systems could also be explained in another way. It is apparent that ϵP_t and/or ϵP_ℓ could be changed in Fig. 4 so as to provide a better fit of Eq. (18) to the data of this study. A lowering of ϵP_t would be particularly effective for this purpose. It is possible that ϵP corresponding to fully mixed void cells in the laminar region could be lower than ϵP for fully mixed cells in the turbulent region. As has been pointed out by Perkins and Johnston[18] such behavior could result from the wider distribution of velocities in the connecting channels in laminar flow. Any realistic mixing cell model must take into account the fact that there is a three dimensional network of cells and connecting channels. In a randomly packed bed it is reasonable to expect that there will be a range in sizes and configurations of void cells and connecting channels. As a consequence there is no reason to expect that the extreme of perfectly mixed cells will give the

same concentration in all cells at a given horizontal bed level at a given time in a dynamic study. The distribution of velocities among the various connecting channels should be wider in laminar flow than in turbulent flow since pressure drop varies with a lower power of velocity. As a consequence cell concentrations at a given bed level would be less uniform than in turbulent flow and ϵP_t would be lower in laminar flow than in turbulent flow.

The data of McHenry and Wilhelm and of Sinclair and Potter coupled with this argument would require that turbulence persist in the connecting channels down to $N_{Re}' = 1$; however the conservation of mass suggests that the connecting channels would have a Reynolds number for flow that is higher than in the cells. As a result many channels might still be turbulent when most of the main cells have become laminar.

It should also be pointed out that the particular weighting factors of ϵ and $1-\epsilon$ in ϵP and N_{Re}' have not been tested for liquids below $N_{Re}' = 10$ and for gases. However the present data, the sphere data of Ebach and White and the results of McHenry and Wilhelm, Carberry and Bretton and Sinclair and Potter were all obtained for random packed spheres with ϵ very nearly equal to 0.4.

C. Dispersion of Heat in Liquids

Any model for the dispersion of mass at low concentrations in a flowing fluid should also be able to handel the dispersion of heat. Green, Perry and Babcock[10] report data for axial dispersion of heat during liquid flow through a randomly packed bed of spheres. Their reported data for water and ethanol, covering a range of Prandtl numbers from 2 to 16, are shown in Fig. 6. The computation of axial dispersion coefficients representing the fluid alone is complex and requires several corrections. The data reported by Green, et al., have been corrected for axial conduction in the solid packing and for convective heat transfer between the fluid and solid. On the other

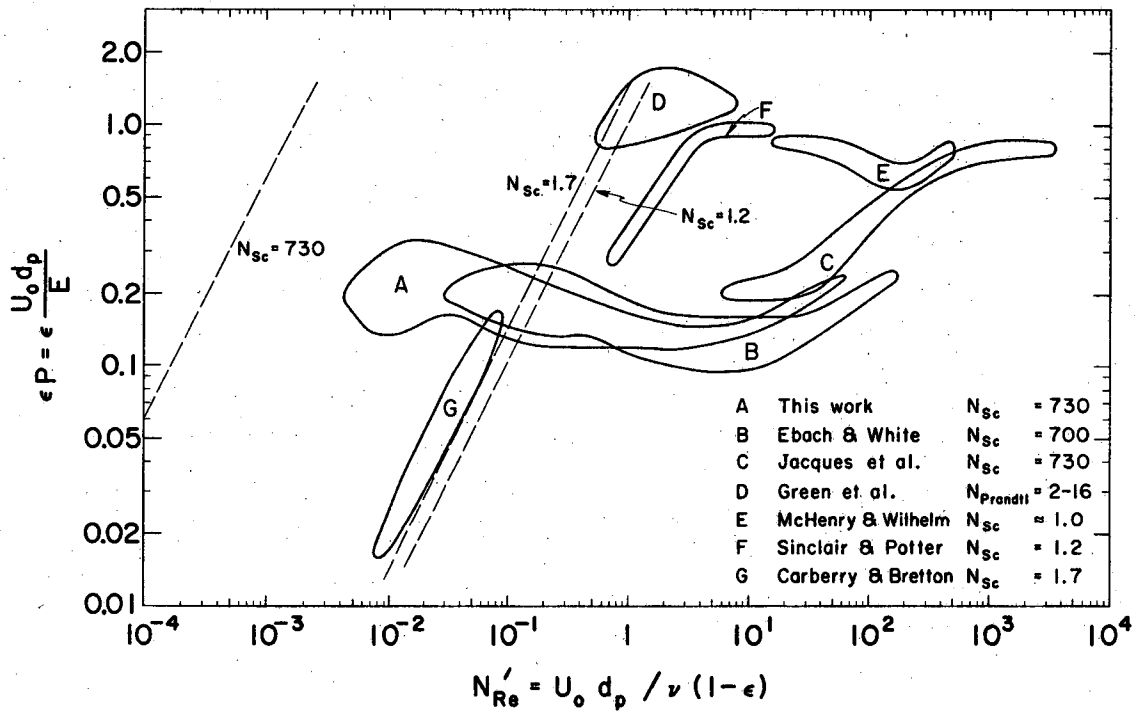

Fig. 6. Comparison with data for mass dispersion in gases and thermal dispersion in liquids.

hand, as the authors point out, no correction could be applied for any effect of radial conduction through the solid packing. The Peclet numbers from Green, et al., shown in Fig. 4 are in a range of N_{Re}' where some turbulence can still exist in the fluid and where eddy and molecular diffusion of heat should be able to keep the main voids well mixed; thus they should be high. The fact that ϵP is even higher than the values of 0.8-0.95 found for mass dispersion in gases may be a symptom of an appreciable leveling out of temperature at a given bed level due to conduction through the packings. Such an effect would be important to the extent that cells at a given level do not have the same temperature at a given time, and its occurrence would lend some credence to the possibility of ϵP_t for mass dispersion in the laminar regime being less than ϵP_t in the turbulent regime. Both these values of ϵP_t would then be less than ϵP_t for heat dispersion with a large solid phase radial thermal conductivity.

D. Effect of Particle Size

The present data exhibit at most a very small effect of particle size on ϵP over a range of a factor of 28 in particle diameter. On this basis it does not seem likely that a particle diameter effect will account for the difference in magnitude of ϵP in gas and liquid systems at the point where an effect due to axial molecular diffusion sets in. Furthermore the gas phase studies of Sinclair and Potter[22] and of McHenry and Wilhelm[16] employed particle diameters similar to those employed in the present study and in the work of Ebach and White.[9] The values of ϵP found by Jacques, et al.[13] for liquids at low Reynolds numbers are in reasonable agreement in magnitude with the data of the present study for the same particle diameter, even though Jacques, et al. employed a much larger bed diameter; hence there appears to be no effect of d_t/d_p.

Some of the seeming effect of particle diameter in past studies of random packed spheres may be ascribable to the fact that it is difficult to obtain a truly uniform sphere diameter in any given bed. Raimondi, et al.[18,19] report that the dispersion characteristics of a bed seem to be governed by the particle diameter corresponding to the 10% cumulative fraction.

ACKNOWLEDGMENT

The authors are grateful for the constant interest and frequent helpful advice of Professor Theodore Vermeulen.

REFERENCES

1. Ampilogov, I. E., A. N. Kharim and I. S. Kurochkina, Zh. Fiz. Khim. 32, 141 (1958).
2. Aris, R., Proc. Roy. Soc. (London), A235, 67 (1956).
3. Beran, M. J., Ph.D. Thesis, Harvard University (1955).
4. Blackwell, R. J., J. R. Rayne and W. M. Terry, Trans. A.I.M.E., 216, 1 (1959).
5. Blackwell, R. J., Soc. Petr. Engrs. J. 2, 1 (1962).
6. Brigham, W. E., P. W. Reed and J. N. Dew, Soc. Petr. Engrs. J. 1, 1 (1961).
7. Cairns, E. J. and J. M. Prausnitz, Chem. Eng. Sci. 12, 20 (1960).
8. Carberry, J. J. and R. H. Bretton, A.I.Ch.E. Journal 4, 367 (1958).
9. Ebach, E. A. and R. R. White, A.I.Ch.E. Journal 4, 161 (1958).
10. Green, D. W., R. H. Perry and R. E. Babcock, A.I.Ch.E. Journal 10, 645 (1964).
11. Harned, H. S. and B. B. Owen, The Physical Chemistry of Electrolytic Solutions, Reinhold, New York (1958).
12. Hennico, A., G. L. Jacques and T. Vermeulen, Chem. Eng. Sci. (to be published).
13. Jacques, G. L., A. Hennico, J. S. Moon and T. Vermeulen, Lawrence Radiation Laboratory Report UCRL-10696, Pt. I, (November 1964).
14. Klinkenberg, A. and E. Sjenitzer, Chem. Eng. Sci. 5, 258 (1956).
15. Liles, A. W. and C. J. Geankoplis, A.I.Ch.E. Journal 6, 591 (1960).
16. McHenry, K. W., Jr. and R. H. Wilhelm, A.I.Ch.E. Journal 3, 83 (1957).
18. Perkins, T. K. and O. C. Johnsont, Soc. Petr. Engrs. J. 3, 70 (1963).
19. Raimondi, P., G. H. F. Gardner and C. B. Petrick, "Effect of Pore Structure and Molecular Diffsuion on the Mixing of Miscible Liquids Flowing in Porous Media," Gulf Res. and Devel. Co., Pittsburgh, Pa., Aug. 31, 1960. Presented at A.I.Ch.E. Annual Meeting, San Francisco, December 1959, Prepring No. 43.
20. Reid, R. C. and T. K. Sherwood, Properties of Gases and Liquids, McGraw-Hill, New York (1958) p. 270.
21. Rifai, M. N. E., Ph.D. Thesis, University of California, Berkeley (1956).

22. Sinclair, R. J. and O. E. Potter, Trans. Instr. Chem. Engrs. 43, T3 (1965).

23. Stahel, E. P. and C. J. Geankoplis, A.I.Ch.E. Journal 10, 174 (1964).

24. Strang, D. A. and C. J. Geankoplis, Ind. Eng. Chem. 50, 1305 (1958).

25. Tompkins, E. R., D. H. Harris, J. X. Khym, USAEC Report AECD-2128, Oak Ridge, Tenn., 1948; J. Am. Chem. Soc. 71, 2504 (1949).

26. von Rosenberg, D. U., A.I.Ch.E. Journal 2, 55 (1956).

NOMENCLATURE

a	Amplitude of the breakthrough curve
C	Concentration
D	Molecular diffusivity
d_p	Particle diameter
d_t	Column diameter
E	Axial dispersion coefficient based on the open bed ($\epsilon E'$)
E'	Mean linear interstitial dispersion coefficient
E_M	Efficiency of mixing in voids over filament mixing
h	Elapsed recorder chart distance between an initial perfect step and the midpoint of the breakthrough
Δh	Recorder chart distance between breakthroughs one and two
K_L	Overall mass transfer coefficient
k_{L_m}	Average mass transfer coefficient for either stream
L	Distance between conductivity cells
m	Constant; d_p/δ
N	Column Peclet number; LU_o/E
n	Constant; u_s/u
N_{Re}	Reynolds number; $U_o d_p/\nu$
N_{Re}'	Corrected Reynolds number; $U_o d_p/\nu(1-\epsilon)$
N_{Sc}	Schmidt number; ν/D
P	Packing Peclet number; $U_o d_p/E$, Ud_p/E'
P_l	Peclet number for infinite N_{Sc} in the laminar regime
P_t	Peclet number for total void mixing
S	Dimensionless midpoint slope = $(h \tan \theta)/a$
$\tan \theta$	Midpoint slope of the breakthrough curve
U	Interstitial velocity
U_o	Superficial velocity
u	Average velocity
u_s	Interfacial velocity (nu)
X	Recorder chart speed
δ	Length of cell side

ϵ	Void fraction
λ	Inhomogeneity factor
ν	Kinematic viscosity

Subscripts

1	Upstream breakthrough point
2	Downstream breakthrough point
i	Entering
o	Exiting
a	Stream a
b	Stream b

APPENDIX I

Data

Run		d_p (cm)	L (in)	T (^oC)	X (in/m)	a_1 (in)	$\frac{9.88}{\tan \theta_1}$	a_2 (in)	$\frac{9.88}{\tan \theta_2}$	Δh (in)	ϵP	N_{Re}'
1	A[a]	.140	22	17.8	15	4.55	0.58	4.68	1.10	1.94	.231	
	C	.140	22	17.8	15	4.41	0.61	4.57	1.13	1.93	.230	
	D[b]	.140	22	17.8	15	4.37	0.50	4.51	1.11	1.93	.221	
											.227	59.8
2	A	.140	22	17.8	15	4.27	1.81	4.43	3.56	5.31	.179	
	B	.140	22	17.8	15	4.27	1.67	4.43	3.52	5.35	.178	
											.179	21.8
3	A	.140	22	17.8	15	4.13	2.88	4.24	5.86	7.95	.159	
	B	.140	22	17 8	15	4.13	2.40	4.24	5.80	8.03	.153	
	C	.140	22	17.8	15	4.13	2.86	4.21	5.90	7.96	.159	
	D	.140	22	17.8	15	4.15	2.65	4.20	5.82	8.03	.162	
											.158	14.5
4	A	.140	22	18.0	15	4.13	3.52	4.24	7.11	9.70	.162	
	B	.140	22	18.0	15	4.13	3.29	4.24	7.31	9.71	.145	
	C	.140	22	18.0	15	4.13	3.35	4.25	7.23	9.63	.147	
	D	.140	22	18.0	15	4.13	3.30	4.25	7.00	9.61	.160	
											.154	12.0

[a] A and C are purge runs.

[b] B and D are injection runs.

Run		d_p (cm)	L (in)	T (°C)	X (in/m)	a_1 (in)	$\frac{9.88}{\tan \theta_1}$	a_2 (in)	$\frac{9.88}{\tan \theta_2}$	Δh (in)	ϵP	N_{Re}'
5	A	.140	22	18.0	15	8.41	3.61	8.49	7.51	20.24	.156	
	B	.140	22	18.0	15	8.56	3.52	8.59	7.55	20.35	.151	
	C	.140	22	18.0	15	8.56	3.71	8.59	7.30	20.16	.166	
	D	.140	22	18.0	15	8.63	3.40	8.58	7.44	20.10	.150	
											.156	5.8
6	A	.140	22	18.0	15	8.75	9.41	8.80	19.90	57.82	.168	
	B	.140	22	18.0	15	8.75	8.58	8.80	19.89	57.22	.162	
											.165	2.0
10	A	.047	22	17.2	15	4.58	3.08	4.60	4.92	10.34	.137	
	B	.047	22	17.2	15	4.59	2.76	4.58	4.81	10.20	.129	
	C	.047	22	17.2	15	4.51	3.18	4.53	5.21	10.61	.129	
	D	.047	22	17.2	15	4.50	2.83	4.54	5.01	10.42	.123	
											.130	3.81
11	A	.047	22	17.2	15	4.55	5.61	4.55	10.48	23.00	.131	
	B	.047	22	17.2	15	4.55	6.13	4.55	10.40	23.30	.149	
	C	.047	22	17.2	15	4.59	5.29	4.59	10.18	22.91	.133	
	D	.047	22	17.2	15	4.59	5.80	4.61	10.44	22.89	.131	
											.136	1.69
12	A	.047	22	17.2	15	8.40	7.27	8.34	12.85	52.92	.145	
	B	.047	22	17.2	15	8.63	5.58	8.54	11.73	51.93	.141	
											.143	0.734

Run		d_p (cm)	L (in)	T ($^\circ$C)	X (in/m)	a_1 (in)	$\frac{9.88}{\tan \theta_1}$	a_2 (in)	$\frac{9.88}{\tan \theta_2}$	Δh (in)	ϵP	N_{Re}'
13	A	.047	22	17.2	2	7.92	1.98	8.01	3.71	15.58	.153	
	B	.047	22	17.2	2	8.08	2.27	8.13	3.70	15.70	.174	
											.164	0.332
14	A	.047	22	17.5	2	8.83	2.52	8.67	4.93	23.73	.170	
	B	.047	22	17.5	2	8.94	2.21	8.80	4.56	23.53	.183	
	C	.047	22	17.5	2	8.90	2.53	8.82	4.81	23.71	.175	
	D	.047	22	17.5	2	8.92	2.21	8.81	4.60	23.54	.179	
											.176	0.218
15	A	.047	22	18.2	2	9.09	3.44	9.06	7.14	38.06	.183	
	B	.047	22	18.2	2	9.08	3.68	9.08	7.24	38.61	.187	
	C	.047	22	18.2	2	9.11	3.36	9.09	7.12	38.50	.183	
	D	.047	22	18.2	2	9.11	3.32	9.08	7.19	38.94	.182	
											.184	0.134
16	A	.047	22	18.2	2	9.17	5.50	9.14	11.89	68.74	.205	
	B	.047	22	18.2	2	9.17	5.61	9.13	11.86	64.78	.216	
	C	.047	22	18.2	2	9.21	5.54	9.14	12.08	70.92	.211	
											.211	0.0742
21	A	.0099	11	22.5	15	4.68	3.38	4.64	5.87	15.93	.134	
	B	.0099	11	22.5	15	4.69	4.50	4.64	5.82	15.97	.152	

Run		d_p (cm)	L (in)	T (^oC)	X (in/m)	a_1 (in)	$\frac{9.88}{\tan \theta_1}$	a_2 (in)	$\frac{9.88}{\tan \theta_2}$	Δh (in)	ϵP	N_{Re}'
21	C	.0099	11	22.5	15	4.69	4.34	4.63	5.70	15.96	.153	
	D	.0099	11	22.5	15	4.68	4.59	4.63	5.16	15.98	.123	
											.141	0.264
22	A	.0099	11	22.5	15	8.45	5.92	8.50	6.95	32.16	.178	
	B	.0099	11	22.5	15	8.45	4.51	8.49	5.95	32.42	.162	
	C	.0099	11	22.5	15	8.46	4.75	8.50	6.06	31.92	.166	
	D	.0099	11	22.5	15	8.47	4.62	8.53	5.84	32.16	.185	
											.173	0.143
23	A	.0099	11	22.5	2	4.70	2.25	4.75	2.97	8.80	.151	
	B	.0099	11	22.5	2	4.73	2.35	4.75	3.04	8.91	.158	
	C	.0099	11	22.5	2	4.72	2.21	4.76	2.76	8.86	.209	
	D	.0099	11	22.5	2	4.78	2.31	4.80	2.98	8.95	.166	
											.171	0.070
24	A	.0099	11	22.5	2	4.79	3.91	4.82	4.99	18.05	.243	
	B	.0099	11	22.5	2	4.78	4.38	4.81	5.37	18.05	.240	
	C	.0099	11	22.5	2	4.79	3.75	4.82	4.78	17.66	.254	
	D	.0099	11	22.5	2	4.79	4.26	4.82	5.41	17.85	.205	
											.236	0.034

Run		d_p (cm)	L (in)	T ($^\circ$C)	X (in/m)	a_1 (in)	$\frac{9.88}{\tan\theta_1}$	a_2 (in)	$\frac{9.88}{\tan\theta_2}$	Δh (in)	ϵP	N_{Re}'
25	A	.0099	11	22.0	2	8.69	3.88	8.66	5.07	37.19	.297	
	B	.0099	11	22.0	2	8.69	4.44	8.66	5.71	37.79	.253	
	C	.0099	11	22.0	2	8.63	3.97	8.66	5.11	36.97	.296	
	D	.0099	11	22.0	2	8.65	4.43	8.66	5.82	37.85	.226	
											.268	0.0165
26	A	.0099	11	22.0	2	8.72	14.01	8.80	16.57	96.0	.279	0.0064
	B	.0099	11	22.0	2	8.78	12.28	8.83	19.25	105.3	.109	0.0058
	C	.0099	11	22.0	2	8.77	12.97	8.85	16.60	110.4	.207	0.0055
	D	.0099	11	22.0	2	8.72	15.00	8.81	20.19	129.7	.196	0.0047
											.198	0.0056
30	A	.0099	22	17.0	15	8.28	5.42	8.32	7.34	45.63	.1029	
	B	.0099	22	17.0	15	8.37	5.05	8.32	7.37	45.42	.0936	
	A	.0099	22	18.5	15	8.55	3.32	8.48	6.20	47.05	.0936	
	B	.0099	22	18.5	15	8.53	3.71	8.51	6.74	48.16	.0860	
											.944	0.18
31	A	.0099	22	18.0	2	8.54	1.13	8.47	1.70	10.47	.0814	
	B	.0099	22	18.0	2	8.60	0.99	8.55	1.50	10.22	.0954	
	A	.0099	22	18.5	2	8.59	0.76	8.55	1.43	10.83	.0935	
	B	.0099	22	18.5	2	8.59	0.68	8.54	1.25	10.63	.1214	
	C	.0099	22	18.5	2	8.55	0.76	8.54	1.38	10.73	.1015	
											.0988	0.102

Run		d_p (cm)	L (in)	T (^oC)	X (in/m)	a_1 (in)	$\frac{9.88}{\tan \theta_1}$	a_2 (in)	$\frac{9.88}{\tan \theta_2}$	Δh (in)	ϵP	N_{Re}'
32	A	.0099	22	18.0	2	8.47	2.15	8.47	2.77	19.48	.154	
	B	.0099	22	18.0	2	8.48	1.73	8.47	2.49	18.16	.122	
											.138	0.056
33	A	.0099	22	18.0	2	8.65	4.55	8.57	6.32	46.98	.135	
	B	.0099	22	18.0	2	8.61	4.38	8.54	5.75	46.23	.142	
	A	.0099	22	18.5	2	8.70	3.11	8.61	5.27	44.68	.128	
	C	.0099	22	18.5	2	8.74	4.62	8.63	6.49	60.37	.205	
	A	.0099	22	18.2	2	8.66	4.26	8.62	6.28	56.18	.171	
	B	.0099	22	18.2	2	8.67	3.29	8.60	6.38	54.66	.115	
	C	.0099	22	18.2	2	8.61	4.13	8.55	6.26	55.14	.161	
											.151	0.023
41	A	.0051	5.5	19.2	15	7.88	6.85	7.83	7.58	23.94	.170	
	B	.0051	5.5	19.2	15	7.88	6.85	7.83	7.58	23.64	.160	
	C	.0051	5.5	19.2	15	7.88	6.31	7.83	7.20	24.14	.144	
	D	.0051	5.5	19.2	15	7.88	6.92	7.83	7.64	23.84	.164	
											.160	0.046
42	A	.0051	5.5	19.2	15	8.98	11.57	8.91	12.80	50.43	.201	
	B	.0051	5.5	19.2	15	8.94	12.18	8.89	13.89	50.28	.129	
	C	.0051	5.5	19.2	15	8.95	11.47	8.90	13.04	50.75	.152	
	D	.0051	5.5	19.2	15	8.95	12.63	8.90	14.52	50.55	.113	
											.149	0.022

Run		d_p (cm)	L (in)	T (°C)	X (in/m)	a_1 (in)	$\frac{9.88}{\tan \theta_1}$	a_2 (in)	$\frac{9.88}{\tan \theta_2}$	Δh (in)	ϵP	N_{Re}'
43	A	.0051	5.5	19.2	2	6.62	3.74	6.45	4.61	13.70	.121	
	B	.0051	5.5	19.2	2	6.62	4.44	6.45	5.09	13.50	.146	
	C	.0051	5.5	19.2	2	6.58	3.88	6.43	4.67	13.52	.126	
	D	.0051	5.5	19.2	2	6.58	4.50	6.43	5.29	13.45	.112	
											.126	0.011
51	A	.0051	22	18.7	2	7.08	2.51	6.64	3.75	32.41	.150	
	B	.0051	22	18.7	2	7.08	2.82	6.64	3.60	32.57	.268	
	C	.0051	22	18.7	2	7.12	2.39	6.59	3.74	32.72	.146	
	D	.0051	22	18.7	2	7.12	2.51	6.59	3.38	32.55	.294	
											.215	0.018
52	A	.0051	22	18.7	2	7.19	4.60	6.67	7.51	67.98	.143	
	B	.0051	22	18.7	2	7.19	5.31	6.67	7.20	68.28	.238	
	C	.0051	22	18.7	2	7.20	4.97	6.68	7.45	68.44	.170	
	D	.0051	22	18.7	2	7.20	5.31	6.68	7.24	68.44	.232	
											.196	0.0086

APPENDIX II

Development of Apparatus

The initial version of the final apparatus was constructed with a nitrogen gas pressure control system. A nitrogen tank followed by pressure regulators served to keep a constant but variable pressure over the two tanks supplying fluid to the column. Copper lines carried fluid through a pair of Brooks (DS 100-2) rotameters to an injection manifold. However, the nitrogen pressure system resulted in a "bends" effect where nitrogen gas was flashed in the rotameters and, far worse, inside the column packing. The small bead size resulted in surface tension effects where gas did not move freely thru the packing. Fear of channeling due to gas pockets in the packing led to replacement of the nitrogen pressure system with constant head tanks (30 feet of water) and also to the very careful packing techniques described below.

Flow rate measurements via rotameter were discontinued because either volumetric measurements of the exit stream of observation of the breakthrough time from the recorder chart supplied better estimates of superficial velocities. Tygon tubing replaced the copper lines because it was easier to put into place. The original injection system utilized the addition of a small amount of tracer solution to a main background stream of water. However, a variety of small problems, ranging from particles getting stuck in the injection needles to too much hold-up of tracer between the injection switch and the injection point, led to the replacement of the tracer system with the final, two stream, manifold design.

The packing operation was always carried out by adding a suspension of beads to a water filled column allowing the beads to settle, and then withdrawing enough water from the top to permit the operation to be repeated.

APPENDIX III

Sample Calculation

Run 3A

d_p = .14 cm.

L = 55.9 cm., 22 in.

ϵ = .4

Δh = 7.95

a_1 = 4.13 in., $\quad 9.88/\tan\theta_1 = 2.88$

a_2 = 4.24 in., $\quad 9.88/\tan\theta_2 = 5.586$

$$\epsilon P_{3A} = \frac{4\pi\epsilon d_p}{L}(9.88)^2 \cdot \frac{(\Delta h)^2}{(a_2 \cdot 9.88/\tan\theta_2)^2 - (a_1 \cdot 9.88/\tan\theta_1)^2}$$

$$= \frac{4(3.14)(0.4)(0.14\text{ cm})(9.88)^2(7.95\text{ in.})^2}{(55.9\text{ cm})[(4.24\text{ in.}\cdot 5.86)^2-(4.13\text{ in.}\cdot 2.88)^2]}$$

$$= 0.159$$

X = 15 in./m

ν = .0115 cm^2/sec at 17.8°C

$$N_{Re}' = \epsilon/(1-\epsilon)\, L\left[(d_p X)/(\nu\Delta h)\right]$$

$$= \frac{0.4}{1-0.4}(55.9\text{ cm})\left(\frac{(.14\text{ cm})\cdot(15\text{ in./m})}{(.0115\text{ cm}^2/\text{sec})(7.95\text{ in.})}\right)\cdot\left(\frac{1\text{ m}}{60\text{ sec}}\right)$$

$$\simeq 1.2$$

ϵP_{3B} = .153

ϵP_{3C} = .159

ϵP_{3D} = .162

$$\epsilon P_3 = \frac{.159 + .153 + .159 + .162}{4} \simeq .158$$